[CANCER RESEARCH 63, 6272–6281, October 1, 2003]

c-MET Mutational Analysis in Small Cell Lung Cancer: Novel Juxtamembrane Domain Mutations Regulating Cytoskeletal Functions[1]

Patrick C. Ma,[2] Takashi Kijima, Gautam Maulik, Edward A. Fox, Martin Sattler, James D. Griffin, Bruce E. Johnson, and Ravi Salgia[2,3]

Department of Medical Oncology [P. C. M., T. K., G. M., M. S., J. D. G., B. E. J., R. S.], and Department of Molecular Diagnostics [E. A. F.], Dana-Farber Cancer Institute, and Department of Medicine, Brigham and Women's Hospital, and Harvard Medical School, Boston, Massachusetts 02115, and Department of Hematology/Oncology, Tufts-New England Medical Center, and Department of Medicine, Tufts University School of Medicine, Boston, Massachusetts 02111 [P. C. M.]

ABSTRACT

Small cell lung cancer (SCLC) is an aggressive cancer, and most patients present with cancer already spread beyond the lung. The receptor tyrosine kinase (RTK) c-MET has been implicated in various solid tumors, including SCLC, and is involved in mediating tumorigenesis, cell motility, scattering, invasion and metastasis. Mutations of c-Met have been described in renal papillary carcinoma and gastrointestinal cancers including hepatocellular carcinoma. The sequence of *c-MET* was examined for possible mutations in the 10 SCLC cell lines and 32 paired-SCLC/normal tissues. Novel *c-MET* alterations were identified among 3 of 10 separate SCLC cell lines and in 4 of 32 SCLC tumor tissue samples. These include two different *c-MET* missense mutations in the juxtamembrane (JM) domain (R988C found in NCI-H69 and H249 cell lines; and T1010I in SCLC tumor sample T31). Also, there are one Sema domain missense mutation (E168D in SCLC tumor sample T5), two-base-pair insertional mutations (IVS13- (52–53)insCT in both SCLC tumor samples T26 and T27) within the pre-JM intron 13, as well as an alternative transcript involving exon 10 (H128 cell line). c-MET receptors are expressed at various levels among the 10 SCLC cell lines studied (high expression: H69, H345, H510, and H526; medium-expression: H128 and H146; and low/no-expression: H82, H209, H249, and H446). The level of c-MET expression does not have any apparent correlation with presence or absence of mutations of *c-MET* in the cell lines. We show that the two identified JM mutations (R988C and T1010I), when introduced into the interleukin-3 (IL-3)-dependent BaF3 cell line, regulated cell proliferation resulting in a small but significant growth factor independence. When introduced into a SCLC cell line (H446, with minimal endogenous wild-type c-MET expression), the JM mutations also regulated cell morphology and adhesion, as well as causing enhanced tumorigenicity by both increases in focus-formation and soft-agar colony-formation assays. Both of the JM mutations also increased cell motility and migration evident in wound healing assay and time-lapse video-microscopy speed analysis. The JM mutations also altered the c-MET RTK signaling, resulting in preferentially increased constitutive tyrosine phosphorylation of various cellular proteins, including the key focal adhesion protein paxillin on tyrosine residue Y31 (first CRKL-binding site), correlating with increased motility. These results suggest a novel and unique role of the JM domain in c-MET signaling in SCLC with significant implications in cytoskeletal functions and metastatic potential. The novel JM gain-of-function somatic mutations described are the first to be reported in SCLC, and may be associated with a more aggressive phenotype. It would now be useful to study the inhibition of c-MET as a therapeutic target against SCLC.

INTRODUCTION

There will be 171,900 projected new cases of lung cancer in the United States in 2003, with ~16% comprised of SCLC[4] (1, 2). It is estimated that there will be 157,200 deaths related to lung cancer for the same year (1). Most patients with SCLC have distant metastases at presentation. Although the majority of patients' primary tumors shrink after the administration of chemotherapy, the median survival remains at 8–10 months and has not changed dramatically in the past 25 years (2, 3). To improve the therapy for SCLC, new potential therapeutic targets are needed.

Both oncogenes and tumor suppressor genes are abnormal in SCLC, including *MYC* DNA amplification, *p53* mutation, *Rb* inactivation, and loss of alleles on chromosome 3p (3). The potential role of RTKs, including c-KIT and c-MET, and its activation in SCLC is of special interest. c-KIT is expressed in SCLC and stimulation of the receptor by its ligand stem cell factor induces cell growth and motility. The small molecule inhibitor STI571 can inhibit the growth of c-KIT-positive SCLC (4, 5). Similarly, *c-MET* has been suggested to be active in SCLC (6, 7). Previous studies have shown that HGF/c-*MET* signaling pathway is functional and important in SCLC (6, 7).

c-MET is a disulfide linked α-β heterodimeric RTK that has previously been identified as a proto-oncogene. The M_r 170,000 precursor c-MET is glycosylated and then cleaved into a M_r 50,000 extracellular α chain and a M_r 140,000 membrane-spanning β chain. c-MET serves as the high-affinity receptor for its natural ligand HGF/scatter factor, referred as HGF thereafter). HGF is a paracrine factor that is produced by stromal and mesenchymal cells, acting on MET-expressing cells (8). Moreover, HGF/c-MET autocrine activation in HGF-transgenic mice *in vivo* with promotion of hepatocarcinogenesis has also been reported (9). Activation of the HGF/c-MET signaling pathway, which requires phosphorylation of various specific tyrosine residues on c-MET itself, leads to cellular responses including increased proliferation, scattering (cell-cell repulsion), increased motility, invasion, and branching morphogenesis (6, 10–13). On ligand binding, c-MET undergoes autophosphorylation of specific tyrosine residues (Y1230/1234/1235) within the activating loop of the tyrosine kinase domain, thereby activating the intrinsic kinase activity of c-MET. Phosphorylation of Y1349 and Y1356 in a cluster of amino acids in the COOH terminus of c-MET activates the multisubstrate signal-transducer docking site ($Y^{1349}VHVX_3Y^{1356}VNV$). Regulation of cell morphogenesis is mediated via Y1365 (6). Within the JM domain, the Y1003 residue has an important role in binding to proteins such as c-Cbl, which can ubiquinate activated c-MET. Moreover, by recruiting the endophilin-CIN85 complex, Cbl regulates c-MET internalization and degradation, thereby having an important functional role in HGF/c-MET signaling regulation (14).

c-MET alterations, including overexpression and mutations, have been well described in a number of solid tumors such as papillary

Received 3/17/03; revised 6/24/03; accepted 7/21/03.

The costs of publication of this article were defrayed in part by the payment of page charges. This article must therefore be hereby marked *advertisement* in accordance with 18 U.S.C. Section 1734 solely to indicate this fact.

[1] Supported by American Cancer Society Scholar Award (to M. S. and R. S.), an American Society of Clinical Oncology (ASCO) Young Investigator Award (to P. C. M.), and an Eastern Cooperative Oncology Group (ECOG)/Ortho-Janssen Biotech Young Investigator Award (to P. C. M.).

[2] Present address: Section of Hematology/Oncology, Department of Medicine, The University of Chicago Medical Center, Pritzker School of Medicine, Chicago, IL 60637.

[3] To whom requests for reprints should be addressed, at Section of Hematology/Oncology, Department of Medicine, The University of Chicago Medical Center, 5841 South Maryland Avenue, Chicago, IL 60637. Phone: (773) 702-4399; Fax: (773) 834-1798; E-mail: rsalgia@medicine.bsd.uchicago.edu.

[4] The abbreviations used are: SCLC, small cell lung carcinoma; NSCLC, non-SCLC; RTK, receptor tyrosine kinase; HGF, hepatocyte growth factor; TLVM, time-lapse video-microscopy; IL, interleukin; JM, juxtamembrane; EGFP, enhanced green fluorescent protein; MTT, 3-(4,5-dimethylthiazol-2-yl)-2,5-diphenyltetrazolium bromide.

renal cancer, gastric cancer, and hepatocellular carcinoma (5–7, 15). Most missense mutations have been found located in the tyrosine kinase domain, and the activating mutation M1268T (exon 19) identified in hereditary and sporadic papillary renal cell cancer causes constitutive activation of the MET tyrosine kinase (16). Identification of the activating mutations of *c-MET* found in hereditary papillary renal carcinomas provides the first direct evidence linking *c-MET* directly to human oncogenesis (16). Germ-line missense mutation in the tyrosine kinase domain (such as M1149T, exon 17; V1206L, exon 18; V1238I, exon 19; D1246N, exon 19; and Y1248C, exon 19; Ref. 16) are detected in the majority of hereditary papillary renal cell carcinomas (17); whereas somatic mutations have been found in some sporadic papillary renal carcinomas (18). For example, 17 of 129 sporadic papillary renal cell carcinomas showed mutations in the *c-MET* gene (such as V1110I, exon 16; H1112L, exon 16; H1124D, exon 16; Y1248D, exon 19). c-MET has been found to be overexpressed in both SCLC and NSCLC, but, thus far, no mutations have been reported in either cancer (6, 7, 15).

We performed mutational analysis of the *c-MET* gene in SCLC, and examined the *c-MET* mutant transfected cell lines for potential functional alterations. Novel somatic missense mutations and alternative splicing isoforms of *c-MET* were identified in SCLC. JM domain mutations of *c-MET* were shown to have activating phenotype with increased cell motility, migration, and tumorigenesis.

MATERIALS AND METHODS

Cell Lines and Cell Culture. The SCLC/NSCLC cell lines (SCLC cell lines NCI-H69, H82, H128, H146, H209, H249, H345, H446, H510, and H526; and NSCLC cell lines A549, H460, H810, H2882, and H3122; Ref. 7), Rat1 fibroblast cell line, and the murine pre-B IL-3-dependent BaF3 cell line (19) were obtained from the American Type Culture Collection (Manassas, VA) and were cultured with 10% (v/v) FCS-containing medium at 37°C with 5% CO_2. BaF3 cells were cultured in the presence of 10% (v/v) WEHI-conditioned medium as the source of IL-3 (19).

Patients and Tumor Tissue Samples. Thirty-two previously described tumor/normal (*T*/*N*) paired samples from SCLC patients were analyzed in the present study (20), in accordance with institutional guidelines.

DNA Sequence Analysis and Primers. The genomic DNA and cDNA from cell lines and tissue samples were prepared by standard procedures. The coding regions in the *c-KIT* and the *c-MET* cDNAs were completely sequenced using standard PCR and sequencing techniques. Genomic DNAs from the 32 paired-SCLC/normal tumor tissue specimens were used to amplify across each exon and some flanking intronic regions. The PCR primer sequences used for the *c-KIT* and *c-MET* mutational analyses are available on request. For analysis of the *TPR-MET* rearrangement in the cDNA from SCLC cell lines; all of the primers used were described previously (21, 22). Sequencing was performed using dye-primer chemistry and the Prism 377 DNA Sequencer (Applied Biosystems). Sequencing was performed with the forward coding strand with confirmation of *c-MET* genomic or cDNA alterations performed by sequencing of the reverse strand as well.

Plasmid Constructs and Site-directed Mutagenesis. Plasmids containing the wild-type full-length *c-MET* cDNA, pRS2 (23, 24), and the *TPR-MET* cDNA insert, pMB23 (25) were generous gifts from Dr. George F. Vande Woude (Van Andel Research Institute, Grand Rapids, MI), and were used for construction of expression plasmid vectors for transfection studies. The respective cDNA inserts were separately subcloned into the bi-cistronic expression vector pIRES2-EGFP (Clontech, Palo Alto, CA), using *Eco*R1 restriction enzyme sites. Using the parental plasmid pIRES2-EGFP containing the subcloned full-length wild-type *c-MET* cDNA insert, JM point mutation (C2962T; or C3029T) of *c-MET* was created using the QuickChange Site-Directed Mutagenesis XL kit (Stratagene, La Jolla, CA) according to the manufacturer's instructions. The point mutation constructs were confirmed by standard DNA sequencing of both strands.

Transfection. H446 SCLC cell line, and Rat1 fibroblast cell line were transfected using the LipofectAMINE PLUS reagent (Life Technologies, Inc., Inc. Rockville, MD) according to the manufacturer's instructions. One μg of expression plasmid DNA, containing either no insert (mock), wild-type c-MET, R988C.Met, T1010I.Met, or the TPR-MET insert, was used for transfection for each 35-mm culture dish. Stable H446 transfected cells were selected by the addition of G418 (100 μg/ml) 3 days after the transfection. Similarly, BaF3 cells were transfected using standard electroporation protocol as described previously (19) with G418 (1 mg/ml) selection for stable clones. Expression of the transfected wild-type or mutated c-MET in the transfected cells was examined by immunoblotting and immunoperoxidase staining using anti-c-MET antibody (C-12, Santa Cruz Biotechnology, Santa Cruz, CA), and the cells were also examined under fluorescent microscopy for expression of the reporter EGFP.

Antibodies and Immunoblotting. The following antibodies were used: antihuman c-MET antibody (C-12, Santa Cruz Biotechnology Biotech, Santa Cruz, CA); antiphosphotyrosine monoclonal antibody (4G10, UBI, Lake Placid, NY); polyclonal phosphospecific pY31-paxillin antibody (Biosource International); anti-paxillin (5H11) antibody (26); and anti-β-actin monoclonal antibody (AC-15, Sigma, St. Louis, MO). Cells were lysed in ice-cold lysis buffer [20 mM Tris (pH 8.0), 150 mM NaCl, 10% glycerol, 1% NP-40, and 0.42% NaF] containing inhibitors (1 mM phenylmethylsulfonyl fluroide, 1 mM Na_3VO_4, 5 μg/ml aprotinin, and 5 μg/ml leupeptin). Cell lysates were separated by 8% SDS-PAGE under reducing conditions and electrophoretically transferred to nitrocellulose membranes (Schleicher & Schuell, Dassel, Germany). Proteins were detected by immunoblotting using an enhanced chemiluminescense technique (NEN Life Science Products, Boston, MA).

Immunoperoxidase Staining. H446 cells stably transfected with *c-MET* or its JM-mutated variants were stained immunohistochemically using antihuman c-MET antibody (C-12; Santa Cruz Biotechnology). Briefly, the stable transfectant cell lines were prepared on glass slides for immunoperoxidase staining by standard cytospin method. The cells were then fixed in ice-cold methanol for 5 min and washed with Tris-buffered saline buffer for 5 min. Quenching of endogenous peroxidase activity was done with incubation in 0.3% H_2O_2 in methanol for 20 min. Subsequent immunoperoxidase staining was performed using standard Vectastain Elite ABC Kit (Vector Laboratories, Inc., Burlingame, CA) according to the manufacturer's instructions.

Cell Morphology and Neurite Structure Analysis. The cells were examined using an Olympus IX70 inverted microscopy, DVC1310 digital video camera, and QED Camera with Standalone 145 software. Digital video images saved were analyzed for morphology with the NIH Image Analysis program (4). The neurite-outgrowth assays were performed on cells seeded at a low cell density (2×10^4 cells/ml) in RPMI growth medium containing 10% FCS. Phase contrast micrographs were then taken on day 6 ($\times$10 magnification lens) in random fields with visible individual cells to be examined. Average number of neurite-like projections per cell as well as the length of them were determined in 20 different single cells chosen from different random views for each of the transfected cell lines by the same investigator.

Cell Proliferation Assay. Cell proliferation assay was performed using standard MTT assay (In Vitro Toxicology Assay kit; Sigma) according to the manufacturer's instructions. Stable cell lines of BaF3 cells, transfected with empty vector (mock), wild-type c-Met, or its JM-mutated variants (R988C.Met and T1010I.Met), and Tpr-Met, were used in MTT proliferation assay with and without IL-3, in the presence of 10% FCS. MTT assay was performed at time 0, 24, 48, and 72 h. At time 0 h, 100 μl of cells at 1×10^4 cells/ml was added to each well of a 96-well plate in quadriplicates according to the above culture conditions. Cells were then incubated at 37°C, 5% CO_2. MTT reagent and solubilization solution were added at the indicated time points, and the plates were read at 570 nM.

Cell Dissociation and Cell Adhesion Assay. G418-selected transfected H446 cells were seeded (2×10^5 cells/ml) in RPMI growth medium containing 10% FCS. Cell suspensions (2×10^4 cells/100 μl) were added to each well of a 96-well plate, with each sample performed in pentaplicates. After 24 h of incubation at 37°C, digital images of the cells were recorded in five random fields for each well using an Olympus IX70 inverted microscope and DVC1310 digital video camera, and QED Camera with Standalone 145 software. Single cells and pairs of cells were counted, with differentiation made between nonadherent round-shaped cells and flattened adherent cells.

Transformation Focus-Formation Assay. H446 cells (3×10^5 cells) were seeded in a 35-mm culture dish and grown to ~80% confluency for transfection with 1 μg of plasmid DNA vector (pIRES2-EGFP), containing

either no insert (mock), or an insert with the wild-type *c-MET*, its JM-mutated variants (R988C.Met or T1010I.Met), and Tpr-Met, using the LipofectAMINE PLUS method as described above. At 48 h after transfection, cells were split at low density into three 100-mm dishes in RPMI medium containing 5% FCS. Cells were fed every 3–4 days and then stained with 0.2% Toluidine blue in 70% ethanol after 2 weeks and foci of >50 cells were counted in triplicates (27).

Soft-Agar Colony-Formation Assay. Anchorage-independent proliferation was examined using Noble agar solution, as described previously (28). Cells were diluted to 5×10^4 cells/ml in 0.4% Noble agar solution in RPMI medium with 10% FCS. Cell suspension (1×10^4 cells/0.4 ml/well) was added to each well of a 24-well plate with an underlayer of 0.8% Noble agar at 37°C, and then were cultured at 37°C for 2 weeks. Twice weekly, 0.4% Noble agar in RPMI with 10% FCS was added (0.3 ml/well) to provide additional nutrients and growth factors. Colonies were counted by the same individual under ×4 low magnification light-microscopy in 3 different nonoverlapping views for each well; this was repeated in triplicate for each point.

Wound Healing Assay. Rat1 fibroblast cells, transfected with wild-type *c-MET* or its mutants, were used in the "wound healing" assay to examine for the alterations of cell motility and migration (29). Cells were initially seeded uniformly onto 60-mm culture plates with an artificial "wound" carefully created at 0 h, using a P-20 pipette tip to scratch on the subconfluent cell monolayer. Microphotographs were taken at 0 h and 15 h. Quantitative analysis of the percentage of wound healing was calculated using distances across the wound ($N = 20$) at 0 h and 15 h, divided by the distance measured at 0 h for each cell line.

TLVM and NIH Image Analysis. Serum-starved (2% FCS) transfected BaF3 cells were placed in uncoated tissue culture plates (35 × 10 mm plates; Becton Dickinson Labware) within an omega temperature-controlled chamber at 37°C, and were examined by continuous video-microscopy using an Olympus IX70 inverted microscopy, DVC1310 digital video camera, and QED Camera with Standalone 145 software. The digital video images were then processed with an Apple Mac computer containing a G4 microprocessor and analyzed with the NIH Image Analysis software program (4).

Quantitative densitometric scanning analysis of the immunoblots was also performed with the NIH Image Analysis program. Protein loading was normalized by adjusting the signal intensity using the β-actin signal. The relative signal intensity ratio is expressed as arbitrary unit (U) after the normalization.

Statistical Analysis. Data are presented with mean values (columns) ± SE (bars). *P*s were determined using two-tailed unpaired Student's *t* test with statistical significance defined as $P < 0.05$.

RESULTS

Novel *c-MET* Mutations in SCLC. We analyzed 10 SCLC (NCI-H69, H82, H128, H146, H209, H249, H345, H446, H510, and H526), 5 NSCLC (A549, H460, H810, H2882, and H3122) cell lines and 32 paired tumor/normal (*T/N* 1–32) tissues from SCLC patients and analyzed the sequence for *c-KIT* and *c-MET* alterations (Fig. 1*A*). A novel JM missense mutation, R988C, was found within exon 14 of both the H69 and H249 cell lines (Fig. 1*B*). Both cell lines were originally derived from patients with extensive-stage SCLC (30). A novel missense mutation E168D (Fig. 1*C*) was identified in exon 2 (Sema domain) in SCLC tissue T5. The DNA from the SCLC tumor sample T31 had another novel JM domain missense mutation T1010I (Fig. 1*D*). These mutations were not found in any of the DNA from the paired-normal samples.

In the H128 cell line, an alternatively spliced *c-MET* transcript, skipping the entire exon 10 (extracellular), was identified (Fig. 1*E*). Finally, identical tumor-specific 2-bp insertions, IVS13-(52–53)insCT, were confirmed within intron 13 (pre-JM domain) in both of the SCLC tumor samples T26 and T27 (Fig. 1*F*). The DNA samples were confirmed to be derived from two different individuals (T26 and T27) by an analysis of five different microsatellite loci on each sample for polymorphisms.

There were no mutations found in the catalytic tyrosine kinase domain in any of the cell lines or SCLC tissues. We also tested five NSCLC cell lines (H460, A549, H810, H2882, and H3122) and found no *c-MET* mutations. No mutations in *c-KIT* were identified in any of the cell lines or tumor samples studied (data not shown). Finally, in none of the cell lines did we detect any expression of *TPR-MET* by reverse transcription-PCR. In regard to identifying polymorphisms, we have used the National Center for Biotechnology Information

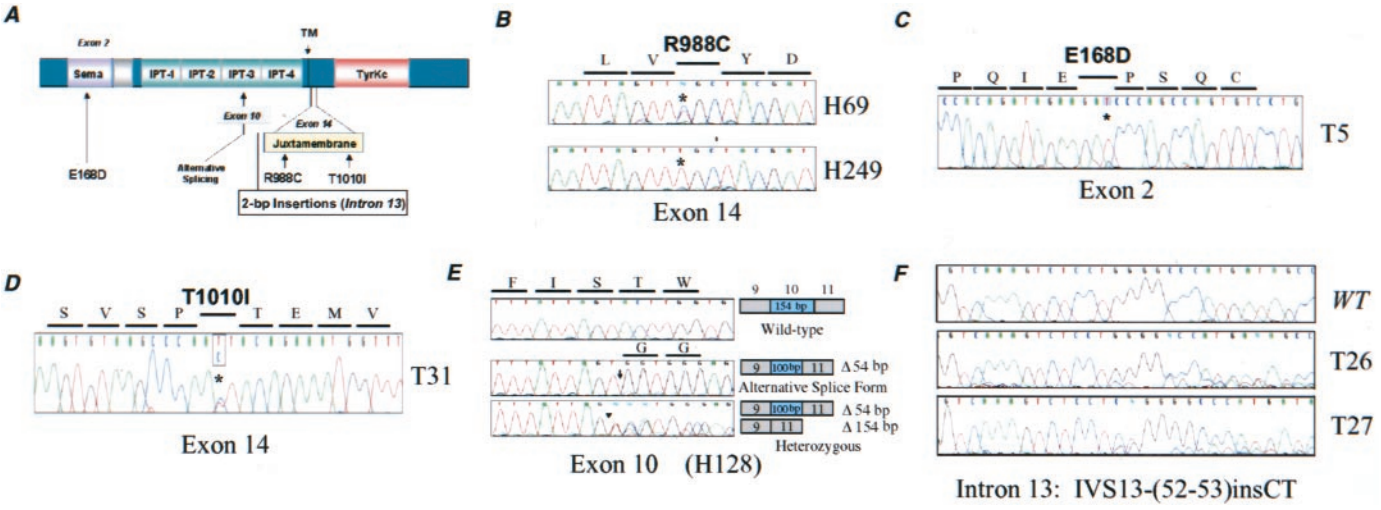

Fig. 1. Novel mutations and alterations of *c-MET* in SCLC. *A*, schematic diagram of the mutations of *c-MET* identified in SCLC. Functional domains with identified mutations of *c-MET* are indicated: Sema domain (*Sema*) at the NH_2 terminus (exon 2) embodied with the MRS (MET-related-sequence) cysteine-rich region; PSI domain, found in plexins, semaphorins and integrins; four IPT repeats, also known as TIG domains, which are found within immunoglobulin, plexins, and transcription factors; the transmembrane (*TM*) and the JM (*Juxtamembrane*) domains; and finally the COOH-terminal intracellular tyrosine kinase (*TyrKc*) domain. *B*, JM missense mutation of *c-MET* cDNA identified in the SCLC cell lines H69 and H249. Point-mutation c.2962C>T (*) resulted in substitution of arginine to cysteine at codon 988 (R988C). The mutation in H69 was heterozygous and that in H249 was homozygous/hemizygous. *C*, Sema domain mutation in SCLC-tissue sample 5 (*T5*). Point-mutation g.504G>T (*) caused a missense substitution from glutamic acid to aspartic acid at codon 168 (*E168D*). *D*, JM missense mutation in SCLC-tissue sample 31 (*T31*). Point-mutation g.3029C>T (*) caused a missense substitution from threonine to isoleucine at codon 1010 (*T1010I*). *E*, alternative splicing involving exon 10 in SCLC cell line H128. The "wild-type" version with the full 154-bp of exon 10 was present at only very low levels (*top panel*). The other two alternatively spliced variants were much more abundant. The second variant spliced species, present in all of the RNAs analyzed, was an alternatively spliced form with the first 54-bp of exon 10 skipped (*middle panel*). The third spliced species identified had exon 10 skipped entirely (*bottom panel*). *F*, two base-pair insertion within intron 13 of the *c-MET* genomic DNA of both tumor samples T26 and T27 [*IVS13-(52–53)insCT*]. Potential alternative splicing skipping exon 14 (JM domain) can be implicated with this specific intronic insertions. *WT*, wild type.

(NCBI) Entrez single nucleotide polymorphism (SNP) database search. None of the mutations of *c-MET* described in this report is present in the polymorphism database, suggesting that they represent somatic mutations. Moreover, we do not see the same mutational changes in the normal counterparts of the paired tumor/normal SCLC specimens, as seen in the tumor tissue. Even though it is still possible that these could represent polymorphisms, our evidence would suggest that they indeed are true missense somatic mutations.

Expression of c-MET in SCLC Cell Lines. We examined the expression of c-MET in the 10 SCLC cell lines used in the mutational analysis by immunoblotting (Fig. 2). c-MET receptor was expressed at various levels among the 10 SCLC cell lines. There was high expression of c-MET in cell lines H69, H345, H510, and H526; medium expression in H128 and H146; and low/no expression in H82, H209, H249, and H446. There does not appear to be any apparent correlation between the level of c-MET expression and whether or not there are any mutations of the receptor. Although both H69 and H345 cell lines have a high expression of c-MET, only H69 cells carry the R988C missense mutation in the JM domain, whereas H345 cells overexpress the wild-type c-MET instead.

Role of JM Domain Mutation of *c-MET* in Cell Proliferation. We focused on the two novel JM mutations of *c-MET* identified, namely R988C and T1010I (Fig. 1, *B* and *D*), to investigate their role in tumorigenesis and biological parameters related to the normal functions of c-MET, such as cell proliferation, adhesion, motility, and migration. JM domain alterations in the RTK Flt3, such as Flt3/ITD, have been reported to induce growth factor-independent cell proliferation when introduced into BaF3 cell line, which is normally IL-3 dependent (31). We investigated the role of JM mutation of *c-MET* in the regulation of cell proliferation and growth factor dependence. We demonstrated that the transforming oncogene *TPR-MET* induces growth factor independence when stably transfected into BaF3 cells, abrogating their normal proliferative requirement of IL-3 (Fig. 3*A*). Of interest, the JM mutations of *c-MET* (R988C.Met and T1010I.Met) also caused a significant IL-3-independent proliferation evident at 48 h, although it was at a lower proliferation rate and was not sustained up to 72 h compared with Tpr-Met.BaF3 cells (Fig. 3*A*). On the other hand, neither the mock-transfected nor the wild-type *c-MET*-transfected BaF3 cells showed any significant IL-3-independent proliferation. In the presence of IL-3, all of the transfected cell lines demonstrated comparable proliferation rates (Fig. 3*B*).

Mutation of the *c-MET* JM Domain Regulates Cell Morphology. We transfected the mutated variants of *c-MET* into the SCLC H446 cell line, which has minimal endogenous c-MET expression and has variant features of SCLC morphology (7, 32). The H446 cell line

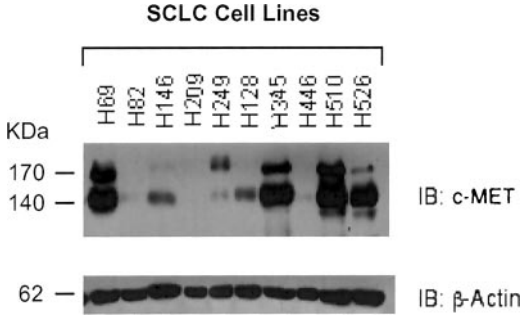

Fig. 2. Expression of c-MET receptor in SCLC cell lines. Whole cell lysates (WCLs) prestarved in 0.5% BSA were prepared from 10 different SCLC cell lines including NCI-H69, H82, H128, H146, H209, H249, H345, H446, H510, and H526. Expression of the c-MET receptor at the protein level was examined by immunoblotting using polyclonal antihuman c-MET antibody (C-12) after the WCLs were separated by 8% SDS-PAGE (*top panel*). The same membrane was stripped and reprobed with β-actin as internal control for protein loading (*bottom panel*). *KDa*, M_r in thousands.

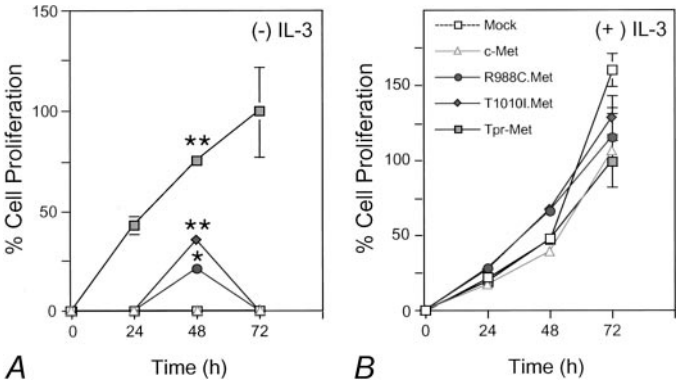

Fig. 3. Mutation of the *c-MET* JM domain modulates growth factor dependence in cell proliferation. BaF3 cells, stably transfected with vector-alone (Mock □), wild-type c-Met (△), its mutated variants R988C.Met (●), T1010I.Met (◆), or Tpr-Met (■), were used in the proliferation assay using standard MTT assay in 10% FCS-containing medium, without (*A*) or with IL-3 (*B*). MTT assay was performed at time 0, 24, 48, and 72 h. In the absence of IL-3, TPR-MET-BaF3 demonstrated autonomous proliferation (100 ± 22.05% at 72 h) characteristic of transformed cells (*A*). Interestingly, a trend of transient IL-3-independent cell proliferation was seen at 48 h in R988C.Met-BaF3 (21.5 ± 3.07%) and T1010I.Met-BaF3 (35.8 ± 3.04%) when compared with the wild-type (c-Met-BaF3: 0%), with $P = 0.0004$ (*) and $P < 0.0001$ (**), respectively. TPR-MET-BaF3 showed IL-3-independent proliferation with 75.2 ± 4.28% already achieved at 48 h, $P < 0.0001$ (**), when compared with the wild-type (*A*). In the presence of IL-3, all of the transfected cell lines exhibited similar proliferation rates (*B*).

grows as a weakly adherent SCLC in cell culture and was originally derived from the pleural effusion of a patient having SCLC with partial response to initial treatment (30). The wild-type *c-MET* and *TPR-MET* were also used as controls for normal function and for activation of c-MET. We studied the morphology and biological functions (tumorigenicity and cell-adhesion) of the H446 cells transfected with *c-MET* or mutated *c-MET* at the JM domain (R988C or T1010I). The transduced expression of the c-MET receptor, or its mutated variants, was shown in the immunohistochemistry staining of the transfectant cells using antihuman c-MET antibody (Fig. 4*A*). H446 cells, transfected with empty vector alone (mock), showed minimal surface staining, whereas the rest demonstrated successful expression of the transfected *c-MET* gene or its JM mutant variants (Fig. 4*A*). There were easily detectable differences in phenotypes, such as cellular patterning, morphology, and cytoarchitecture in H446 cells transfected with JM mutation of c-MET compared with H446 transfected with wild-type *c-MET* or vector alone (Fig. 4*B*). The relative ratio of neurite-like projections per cell in H446 transfected with the JM mutants (R988C: 1.46, $P < 0.045$; T1010I: 1.32, $P < 0.035$) was significantly higher than the value of H446 cells transfected with the *c-MET* gene with normal sequence (c-Met: 1.22; Fig. 4*C*). There was also a significant increase in the neurite-like projections length measured as relative neurite-length index (R988C: 1.85, $P < 0.046$; T1010I: 2.14, $P < 0.003$), compared with c-Met-H466 cells (1.60; Fig. 4*D*).

JM Domain Mutation of *c-MET* Regulates Cell Adhesion. We found that c-Met-H446 cells (transfected with wild-type *c-MET*) exhibited significantly enhanced cell-spreading and adherent phenotype (% adherence, 73.6%; $P < 0.0001$) compared with H446 transfected with vector alone (% adherence, 23.6%; Figs. 4*B* and 5*A*). In contrast to c-Met-H446, R988C.Met-H446, and T1010I.Met-H446, cells showed less cell-spreading (Fig. 4*B*). R988C.Met-H446 (33.2%; $P < 0.0001$) and T1010I.Met-H446 (38.4%, $P < 0.0001$) cells also demonstrated less cell-adhesion than H446 transfected with the wild-type *c-MET* gene (Fig. 5*A*).

JM Domain Mutation of *c-MET* Induces Cell Motility and Migration. The JM mutations of *c-MET* were then studied for their impact on cell motility and migration. We first used the adherent Rat1

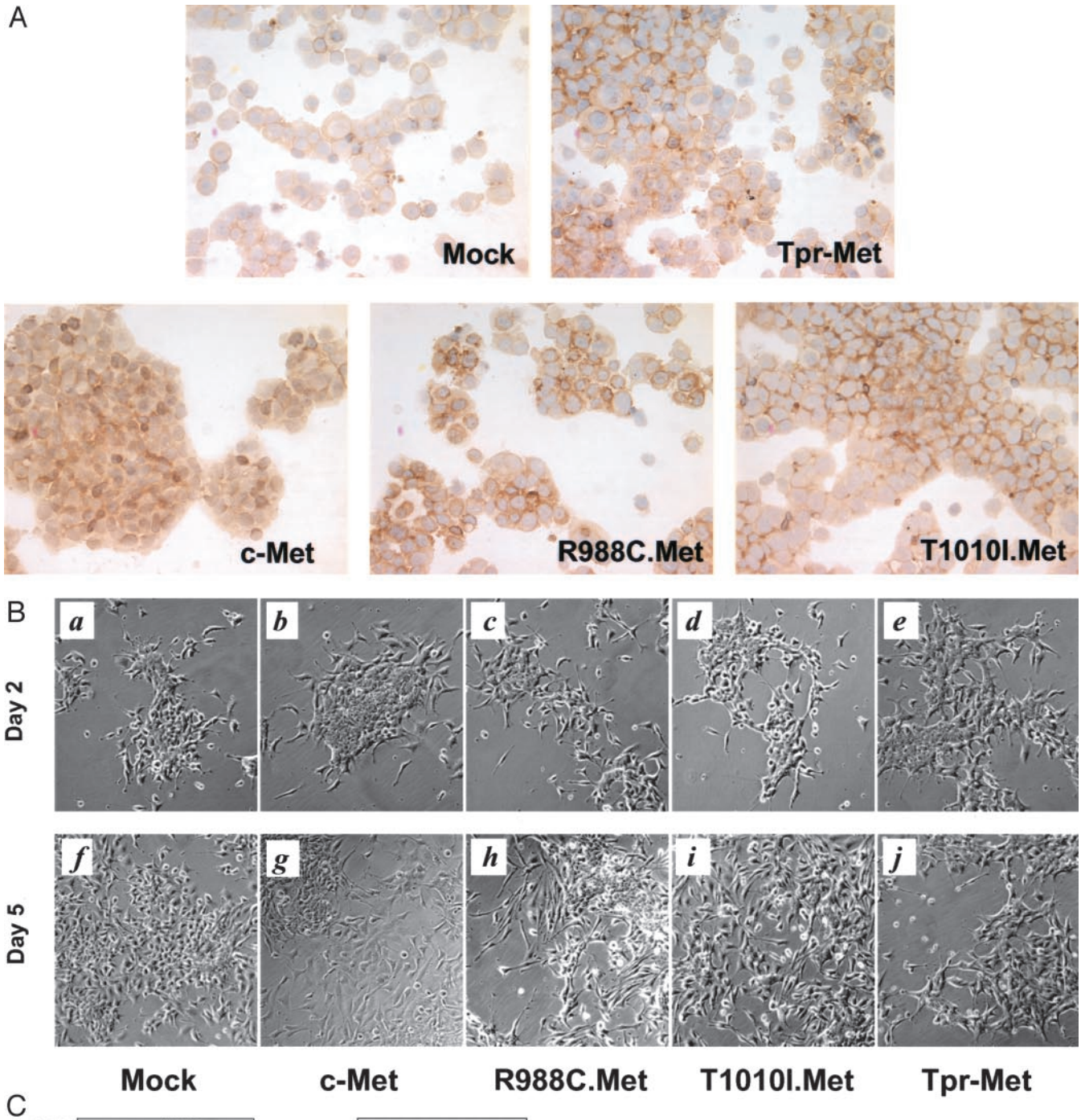

Fig. 4. Mutation of the *c-MET* JM domain regulates cell morphology in H446 cells. *A*, transduced expression of the *c-MET* gene or its mutated variants in SCLC H446 cells. H446 cells transfected with vector-alone (*Mock*), wild-type c-MET or its mutated variants (*R988C.Met*, *T1010I.Met*, or *TPR-MET*) were prepared on glass slides using cytopsin. Standard immunoperoxidase staining was performed using the polyclonal anti-c-MET antibody (C-12) as described in "Materials and Methods." *B*, alteration of phenotype (cellular morphology, patterning, and cytoarchitecture) in H446 cells transfected with *c-MET* and its JM mutants. Cellular patterning and cytoarchitecture at day 2 (*a–e*) and day 5 (*f–j*) after uniform cell seeding at low cell density in tissue culture flasks are shown. Mock-H446 serves as control (*a, f*). c-MET-H446 (*b, g*) showed impressive cell-spreading, orderly cellular patterning and cytoarchitecture. In contrast, R988C.Met-H446 (*c, h*) and T1010I.Met-H446 (*d, i*) cells showed increased cell polarity, less prominent cell spreading, and a more disorderly cellular patterning and cytoarchitecture different from TPR-MET-H446 cells (*e, j*). *C*, neurite-like projections in H446 transfectants. *Left*, the number of neurite-like projections in H446 transfectants was represented as relative ratio (average number of neurite-like projections per cell in experimental cells/average number in mock-H446 cells × 100%). *Right*, the length of neurite-like projections in H446 transfectants was represented as the relative neurite-length index (average length in experimental cells/mock-H446 cells × 100%).

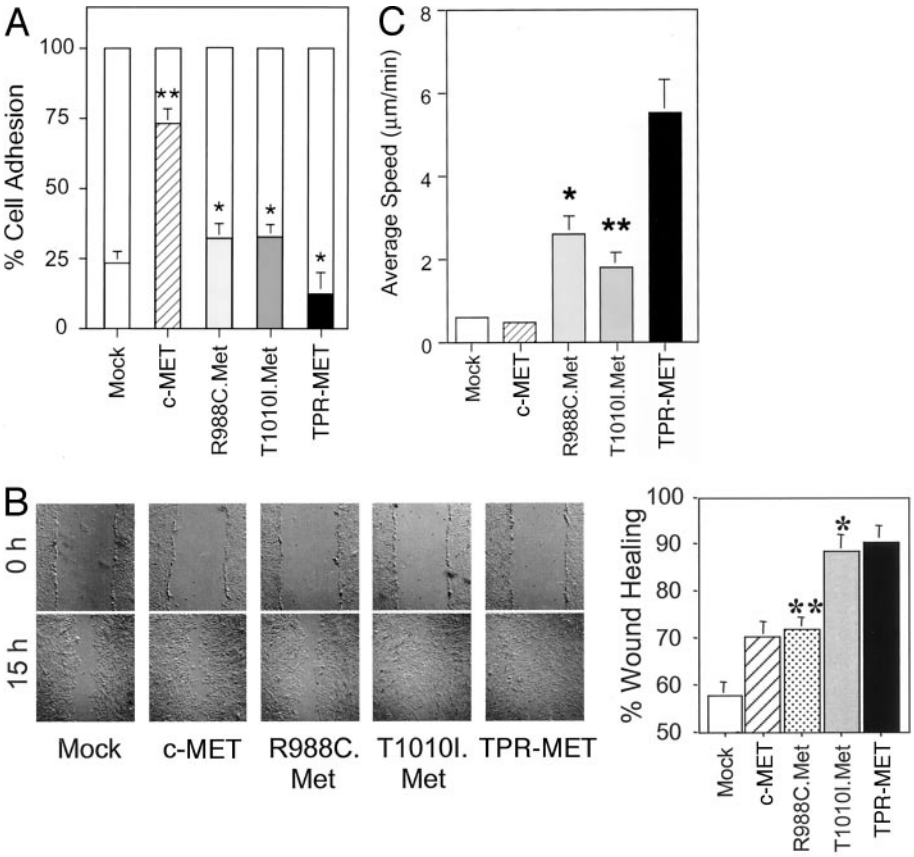

Fig. 5. Mutation of the *c-MET* JM domain regulates cytoskeletal functions: adhesion, motility, and migration. *A*, cell adhesion and dissociation assay. After 24 h of incubation at 37°C, digital images of the cells were recorded in five random fields for each well (see "Materials and Methods"). Single and pairs of cells were counted, also differentiating between nonadherent round-shaped cells and flattened adherent cells. Percentage of cells, single or in pairs, that were adherent among the dissociated cells was represented for each cell line. c-MET-H446 cells exhibited significantly enhanced cell-spreading and adherent phenotype (** % adherence = 73.6%, $P < 0.0001$) compared with H446 transfected with vector alone (% adherence = 23.6%). R988C.Met-H446, and T1010I.Met-H446 cells, in contrast to the wild-type, showed less cell spreading and less cell adhesion. Percentage (%) cell adhesion for R988C.Met-H446 was 33.2% (* $P < 0.0001$) and for T1010I.Met-H446 was 38.4% (* $P < 0.0001$), both significantly less than that of the wild type. *B*, motility and migration analysis by wound healing assay. *Left*, Rat1 cells, transiently transfected with wild-type *c-Met* or its mutated variants, were used in the wound healing assay. Digital pictures were taken then at 0 h as well as at 15 h. *Right*, quantitative results are shown as wound healing index, which was calculated using 20 randomly chosen distances across the "wound" at 0 h and 15 h as described in *Materials and Methods* for each cell line. Increase in wound healing index seen in T1010I.Met-Rat1 cells (*) in comparison with wild-type c-Met-Rat1 is statistically significant ($P = 0.0012$). The difference between R988C.Met-Rat1 (**) and the wild-type does not reach statistical significance ($P = 0.062$). *C*, motility analysis by TLVM. BaF3 cells, transfected with empty vector (*Mock*), wild-type c-Met, or its JM-domain mutated variants, were prestarved with medium containing only 2% FCS for 3 h and then were examined under continuous TLVM. Motility analysis was subsequently performed on the saved digital images with the NIH Image Analysis software program. Speed of motility/migration was calculated by tracing the centroid position of each individual cell every 2 min for a total of 20 min. Speed value (μm/min) from each individual cell was then calculated by dividing the total distance traversed (μm) by the time lapsed, and 20 individual cells were used for each cell line to calculate the average speed. *Error bar*, the SE from 20 speed measurements in each cell line; *, $P = 0.0013$ for R988C.Met-BaF3 when compared with the wild-type c-Met-BaF3 cells; **, $P = 0.0014$ for T1010I.Met-BaF3 when compared with the wild-type c-Met-BaF3 cells.

fibroblast cell line for transfection to study cell motility and migration using an *in vitro* wound healing assay (Fig. 5*B)*. At 15 h, there was significantly more motility and migrational movements with the T1010I mutation (wound-healing index, 88.6%; $P = 0.0012$) compared with the wild-type (c-MET, 70.4%; Fig. 5*B*). With the R988C mutation, the percentage wound healing (72.0%, $P = 0.69$) was slightly greater than with the wild-type *c-Met* (70.4%, $P = 0.0091$), which in turn also has higher than baseline motility seen with Rat1 cells transfected with vector alone (mock, 57.9%).

Alternatively, we also examined the effects of serum-starvation (2% FCS) on cell motility under TLVM, in the context of the *c-MET* JM mutations using the BaF3 cells transfected with wild-type or the JM-mutated variants of *c-MET* (Fig. 5*C*). The cell motility was measured as the average speed of migration of the cells in culture, which was calculated using the distance traversed by the centroid coordinate of each cell over a period of 20 min with the aid of the NIH Image Analysis software. It was found that the average speed of migration of BaF3 cells transfected with wild-type c-Met was 0.5057 ± 0.0516 μm/min ($n = 20$); whereas that of R988C.Met and T1010I.Met-transfected BaF3 cells were both higher at 2.6049 ± 0.4397 μm/min ($n = 20$) and 1.8139 ± 0.3499 μm/min ($n = 20$) respectively. Little motility was noted when the mock-transfected BaF3 cells were examined under the same condition, with the average speed being only 0.6093 ± 0.0609 μm/min ($n = 20$). *TPR-MET*-transfected BaF3 cells, on the other hand, exhibited the most motility with the average speed of migration at 5.5173 ± 0.7868 μm/min ($n = 20$).

JM Domain Mutation of *c-MET* Enhances SCLC Tumorigenicity *in Vitro*. SCLC H446 cell lines transfected with JM mutated *c-MET* (R988C.Met-H446 or T1010I.Met-H446) were compared with those transfected with vector alone (Mock-H446) or with the wild-type c-*MET* (c-MET-H446) sequence, using focus-formation assay and soft-agar colony-formation assay. Wild-type c-MET-H446 cells had significantly increased focus-formation (138.3%, $P < 0.022$) and also soft-agar colony-formation (216.4%, $P < 0.012$; Fig. 6) compared with H446 cells transfected with vector alone (100%). Further increase in focus-formation was seen in both JM mutants (R988C: 179.4%, $P < 0.018$; and T1010I: 176.5%, $P < 0.026$) when compared with c-MET-H446 (138.3%; Fig. 6*A*). Similarly, there was a small but

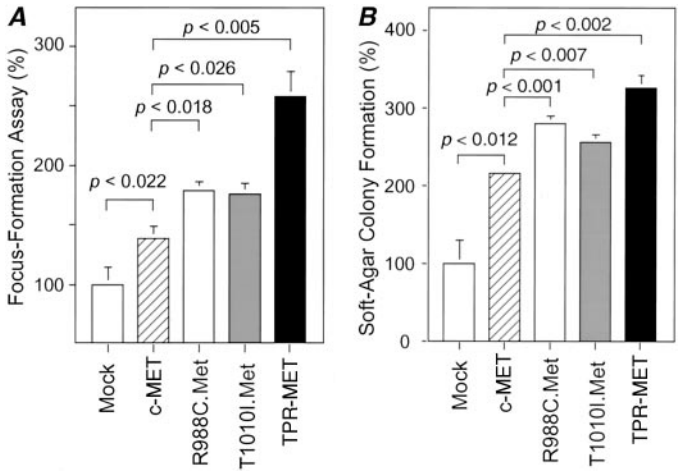

Fig. 6. Mutation of the JM domain of *c-MET* enhances *in vitro* tumorigenicity. *A*, JM mutation of *c-MET* increases focus formation in SCLC H446 cells. H446 cells were transfected with empty vector (*Mock*), wild-type c-Met, or its JM mutated variants (*R988C.Met* and *T1010I.Met*) in a transformation focus-formation assay as described in "Materials and Methods." Tpr-Met-transfected H446 cell line was used as positive control. *B*, JM mutation of *c-MET* increases anchorage-independent proliferation of H446 cells. H446 cells, stably transfected with empty vector (Mock), wild-type c-Met, or its JM mutated variants (*R988C.Met* and *T1010I.Met*), were used in a soft-agar colony-formation assay as described in "Materials and Methods." Tpr-Met-transfected H446 cell line was included as positive control.

significant increase in anchorage-independent growth among the JM-mutated variants of c-MET (R988C: 281.4%, $P < 0.001$; and T1010I: 256.8%, $P < 0.007$) compared with the wild-type c-Met-H446 (216.4%) by soft-agar colony-formation assay (Fig. 6*B*).

Novel Role of JM Domain Mutation in c-MET Signaling and Downstream Target Paxillin. To examine the effects of JM mutation on c-MET signaling and tyrosine phosphorylation, we also performed transfection studies with BaF3 cells. The two JM mutant-transfected cell lines (R988C.Met-BaF3, and T1010I.Met-BaF3) exhibited preferentially increased constitutive tyrosine phosphorylation of various cellular proteins (Fig. 7), compared with wild-type *c-MET* transfected cells. Tpr-Met-BaF3, serving as the positive control, showed the highest levels of constitutive tyrosine phosphorylation of cellular proteins. After adjusting for the levels of expression of the transduced c-MET or JM mutant MET, and also normalization for protein loading using β-actin immunoblot signal, the relative levels of tyrosine phosphorylation of various cellular proteins are represented in Fig. 7*B*. In summary, the constitutive phosphotyrosine levels of the cellular proteins analyzed (*rows A–E*, as shown in Fig. 7*A*) are 5–10-fold higher in the JM mutant MET (R988C.Met and T1010I.Met) than in the wild-type c-MET (*WT*).

To further study the effects of the two missense JM *MET* mutants on cytoskeletal signaling, we examined the tyrosine phosphorylation of the key focal adhesion cytoskeletal protein paxillin, using the phosphospecific antibody directed against paxillin at the amino acid residue Y31 (the first CRKL-binding site). We have previously shown that tyrosine phosphorylation of paxillin at pY31 can be induced by the c-MET ligand HGF in SCLC (7). The levels of constitutive phosphorylation of tyrosine residue 31 on paxillin (pY31) were preferentially induced in R988C (1.27-fold) and T1010I (1.88-fold), with the wild-type signal normalized at arbitrary unit 1.0 U (c-Met-BaF3; Fig. 8).

DISCUSSION

We show in this study that there are unique missense mutations in *c-MET* in SCLC. The novel Sema and JM domain missense mutations of *c-MET* identified in the present study are the first to be reported in SCLC. Aberrant c-MET signaling has been described in a variety of human cancers (6, 15). Although there have been mutations of *c-MET* reported in a variety of solid tumors, the majority of the previously reported mutations were found within the catalytic tyrosine kinase domain as activating missense mutations (15). There have not been any previous reports on activating mutations of *c-MET* in SCLC. No alterations of *c-MET* within the catalytic tyrosine kinase domain were detected in any of the 10 SCLC cell lines and 32 paired-SCLC tumor specimens. *c-MET* was originally identified as the normal counterpart of the fusion oncogene *TPR-MET* (M_r 65,000), which was a result of chromosomal rearrangement in which the *TPR* locus (translocated promoter region, chromosome 1) was translocated to just upstream of the cytoplasmic portion of the *MET* gene (chromosome 7) after treatment of a human HOS cell line with *N*-methyl-*N*′-nitro-*N*-

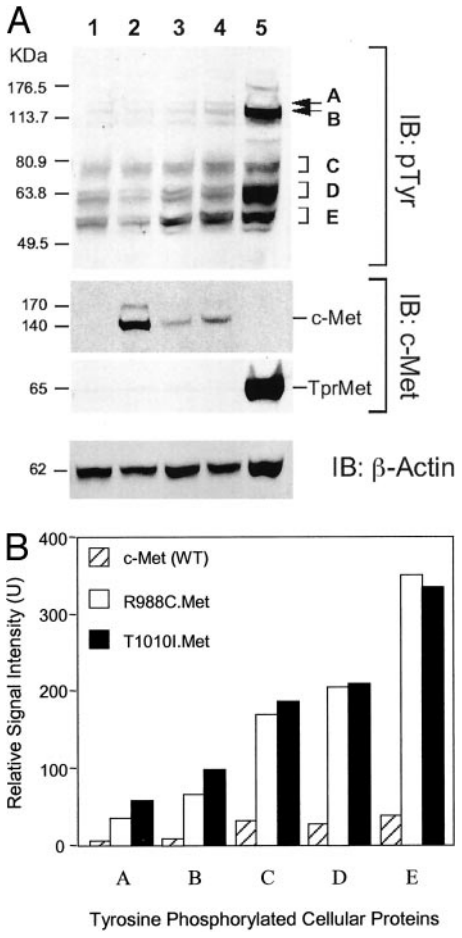

Fig. 7. JM mutation of *c-MET* alters signaling through increased tyrosine phosphorylation of cellular proteins. *A*, *top panel*, whole cell lysates from prestarved BaF3 cells transfected with wild-type *c-Met* (*Lane 2*), or its JM-mutated variants (R988C.Met, *Lane 3*; and T1010I.Met, *Lane 4*), were separated by 8% SDS-PAGE and were transferred to Immobilon-membrane for immunoblotting with antiphosphotyrosine (*IB: pTyr*) antibody. Whole cell lysates from cells transfected with vector-alone (*Mock, Lane 1*) and *Tpr-Met* (*Lane 5*) were used as controls. The same membrane was then stripped and reprobed with antihuman c-MET (*IB: c-Met*) antibody (*middle panel*) and anti-β-actin (*IB: β-Actin*) antibody (*lower panel*), respectively. The results were reproducible in duplicate immunoblots. *B*, preferential induction of tyrosine phosphorylation of cellular proteins by the JM mutations of *c-MET*. The phosphotyrosine immunoblot as shown in *A* (*top panel, A*) was analyzed quantitatively using the NIH Image Analysis software program. The relative signal intensities of tyrosine phosphorylated cellular proteins band(s) (*Lanes A–E*) of the wild-type c-Met, R988C.Met, and T1010I.Met whole cell lysates were determined using the NIH Image Analysis program. Similarly, the signal intensities of the anti-β-actin immunoblot (*bottom panel, A*) and anti-c-Met immunoblot (*middle panel,* A) were obtained and used for the normalization of protein loading and transfected c-Met/JM-Met mutants expression levels, respectively. The relative signal intensity ratio is expressed as arbitrary unit (*U*) after the normalization. *KDa*, M_r in thousands.

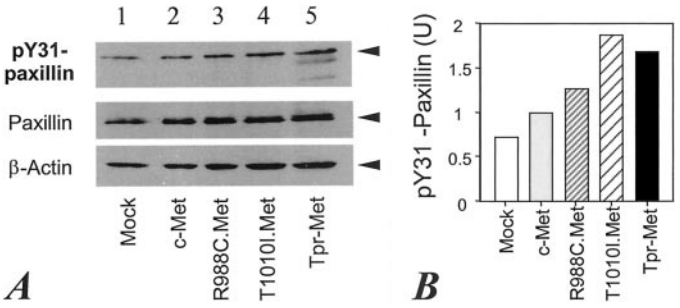

Fig. 8. Relative level of pY31-paxillin tyrosine phosphorylation in JM mutants of *c-MET*. *A*, whole cell lysates of BaF3 stable transfectants of wild-type c-Met (*Lane 2*) or its mutants (R988C.Met, *Lane 3*; and T1010I.Met, *Lane 4*) as detected in immunoblotting with phosphospecific anti-pY31-paxillin antibody. Whole cell lysates from cells transfected with vector-alone (*Mock*, *Lane 1*) and *Tpr-Met* (*Lane 5*) were used as controls. The results were reproducible in duplicate immunoblotting experiment. The same membrane was then stripped and reprobed with anti-paxillin monoclonal antibody (5H11) and anti-β-actin antibody. *B*, the relative pY31-paxillin levels were then quantitated with densitometric scanning, adjusted for protein loading with β-actin signal normalization. The relative pY31-paxillin level was then expressed as relative signal intensity using the wild-type c-Met (*Lane 2*) as normal standard (1.0 U).

nitrosoguanidine (33). *TPR-MET* expression has been reported to be present in gastric carcinoma, namely in 4 of 4 cell lines and in biopsy samples from 12 of the 22 patients (34). TPR-MET is constitutively phosphorylated, with activated MET kinase activity. We did not find any evidence of expression of *TPR-MET* in the 10 SCLC cell lines in this study.

Two different missense mutations have been detected in the JM domain of c-MET in the present study. The JM domains of RTKs have been shown to be key regulators of catalytic functions of the kinases (35–38). As an example, the structural basis for auto-inhibition of EphB2, a member of the largest known family of human RTKs, by the unphosphorylated JM region, has recently been delineated. Phosphorylation of the conserved JM tyrosines residues of EphB2 relieves this auto-inhibition, allowing the ligand-induced autophosphorylation of the tyrosine residues in the cytoplasmic catalytic kinase domain to take place (35). The oncogenic *TPR-MET* lacks the entire JM domain of wild-type *MET* as a result of the chromosomal translocation. When transfected into BaF3 cells, *TPR-MET* caused cellular transformation of BaF3 cells, resulting in abrogation of the normal IL-3 dependence in proliferation. Besides this growth factor autonomy, *TPR-MET* also induced dramatic increase in tumorigenicity and constitutive tyrosine phosphorylation of cellular proteins, correlated with a significant positive modulation of cell motility and migration. Interestingly, the JM mutation of *c-MET* in the present study showed an overall positive gain-of-function activating effect on various parameters, such as growth-factor-independent proliferation (albeit transient), tumorigenicity, and altered *c-MET* signaling with enhanced tyrosine phosphorylation, as well as enhanced cell motility and migration. The JM mutation of *c-MET* demonstrated activating effects on these biochemical and biological functions significantly greater than the wild-type counterpart.

We present evidence that the c-MET JM mutations R988C and T1010I disrupt wild-type c-MET RTK signaling, with enhanced constitutive protein tyrosine phosphorylation. The JM mutations are associated with altered phenotypic changes, including alterations of morphology and adhesion, as well as increased *in vitro* tumorigenicity in SCLC. These phenotypic alterations are potentially correlative of an increased metastatic phenotype. Neurite-like projections and a more pronounced neuroendocrine differentiation of tumors have been associated with an invasive and metastatic phenotype (39, 40). Implication for increased tumorigenicity with the *c-MET* JM mutation (R988C.Met and T1010I.Met), conferring an advantage in tumor progression, was evident. In correlation with the findings of positive induction of cell motility and migration by the JM mutations, our results suggest that the altered motility likely has a significant impact on the metastatic potential of the SCLC tumor cells carrying JM mutation of *c-MET*. Hence, it would be important to determine through *in vivo* models the significance of the JM domain of the HGF/c-MET pathway in metastasis. Selection of somatic mutations of c-MET within the tyrosine kinase domain has been identified during metastasis (41), but thus far, little has been reported within other functional domains. T1010I has been previously considered potentially as a rare germ-line "polymorphism" when identified in a tumor biopsy of hereditary renal papillary cancer and a papillary renal carcinoma cell line ACHN (18). In a study by Schmidt *et al* (18)., when this mutation was introduced into NIH3T3 cells, there was no increased focus formation or increased constitutive *c-MET* phosphorylation. This mutation has also been detected in the large-cell lung cancer cell line Hop-92 and in a patient with breast cancer (28). Lee *et al.* (28) have shown that in athymic nude mice, tumors formed slightly faster with T1010I than with wild-type c-MET. Our report here provides evidence that T1010I, like R988C, does not simply represent a germ-line polymorphism in SCLC. Of interest, another novel germ-line missense mutation P1009S (exon 14) that affects the JM domain of *c-MET* has been detected in a patient with gastric carcinoma, but it was not constitutively activating the c-MET RTK. However, P1009S-mutated *MET* caused colony formation in soft agar, were tumorigenic in athymic nude mice, and also showed increased and persistent tyrosine phosphorylation on HGF stimulation when expressed in NIH3T3 cells (28).

We have further identified paxillin, a key focal adhesion cytoskeletal protein, as one candidate target cellular protein with preferentially enhanced constitutive tyrosine phosphorylation induced in R988C.Met and T1010I.Met. These results strongly imply a unique role for the JM mutations in modulating SCLC cytoskeletal signaling and functions. Cytoskeletal functions are mediated by a host of cytoskeletal proteins, including the most abundant member actin filament, and other accessory proteins such as integrins and focal adhesion proteins (42, 43). Paxillin is a M_r 68,000 adapter protein that contains LD motifs, LIM domains, Src-homology 2 (SH2), and SH3-binding domains that can serve as docking sites for cytoskeletal proteins, tyrosine kinases such as Src, serine/threonine kinases, GTPase activating proteins, and other adapter proteins (actin, vinculin, Crk/CRKL; Ref. 42). Together with other focal adhesion proteins, paxillin is involved in organization and function of focal adhesions, which are critical to cell adhesion and migration. Paxillin signaling also converges with the Rho-dependent signaling pathway in regulating cell motility. We have previously shown that HGF/c-MET signaling induces tyrosine phosphorylation of paxillin in SCLC, and specifically at the tyrosine residue pY31 (first CRKL-binding site) but not pY118 (Crk-binding site) or pY181.

JM domain alternative splicing is potentially an important mechanism modulating c-MET signaling and at least three 8-kb c-*MET* mRNA variants presumably generated through alternative splicing have been reported (44). The 2-bp insertions that we identified in the pre-JM intron 13 (T26 and T27) can potentially cause alternative mRNA splicing, via the splicing mechanism subgroup that generates the type I exon deletion (45), skipping the entire JM domain (exon 14) of c-*MET*. Genome-wide analysis of alternative splicing reveals that 40–60% of all human genes have alternatively spliced isoforms (46). In addition, genome-wide computational screening has also identified the existence of tumor-associated alternative RNA splicing isoforms in human cancers (45). In mouse tissues, a shorter isoform transcript of *c-MET* (c-Met_{sm}), formed through mRNA alternative splicing, has been reported, which had an in-frame deletion of 47 amino acids in the

JM domain (47). The deletion of the JM region leads to increased tyrosine phosphorylation of cellular proteins and enhances the association of c-MET with the p85 subunit of phosphatidylinositol 3′-kinase (48). It would now be useful to search for this unique JM-deleted isoform, which is potentially tumor-associated, and we have started a wider scale of mutational analysis of lung cancer tumor tissue cDNA samples.

Within exon 2 (Sema domain) of the SCLC tumor tissue T5, the point mutation identified, g.504G>T, resulted in the E168D missense substitution. The NH_2 terminus Sema domain is conserved among all semaphorins and is also found present in the plexins (semaphorins receptors) and c-MET. Semaphorins are a large family of secreted and transmembrane signaling proteins regulating neuronal axonal guidance and mediating scattering signaling in epithelial cells. Recent studies also support a role for semaphorins in lung branching morphogenesis (49). Interestingly, aberrant semaphorin signaling may have a role in SCLC tumor progression, as implicated previously with findings of homozygous deletion of 3p21.3, in which the genes for Sema 3B and Sema 3F are located, in several SCLC cell lines (49–51). Thus, it would be useful to further determine the functional implication of the E168D mutation in SCLC. We also found evidence of alternative transcripts of *c-MET* involving exon 10 (H128), the biological significance of which is unclear at present. Alternative splicing within exon 10 has been described as generating a c-MET isoform with an 18-amino-acid deletion in the extracellular region, which is the most abundant variant in a variety of tissues and cell lines (44). Although we focused on the JM mutations of *c-MET* in this report, transfection studies to investigate the effects of the Sema domain mutation and alternatively spliced variants of *c-MET* are currently in progress in our laboratory.

Although the total number of novel *c-MET* alterations, including the JM mutations, identified in our present study appears to be of a small percentage, they may still be of clinically significant relevance and have therapeutic implications. Various *c-MET* mutational alterations may confer different degrees of susceptibility to molecularly targeted therapeutic agents. As an example, Morotti *et al.* (52) recently reported the natural alkaloid kinase inhibitor K252a, with various activities against Trk and the platelet-derived growth factor receptor, is also active against c-MET. Of particular interest, the inhibitor apparently is more potent against the strongly activating form of MET, M1268T, than against the wild-type MET (52). It would also be useful in the future to examine a multitude of tumor tissue specimens to better estimate the frequency of *c-MET* mutations in SCLC. We have recently demonstrated that TPR-MET tyrosine kinase can be inhibited with apoptosis induction by a small-molecule selective c-MET inhibitor, SU11274 (53). We can now use this c-MET tyrosine kinase inhibitor to test against the various *c-MET* JM mutations in SCLC. Taken together, our results suggest a novel role of the JM domain in c-MET signaling, and in promoting SCLC tumorigenicity and tumor cell motility and migration. The altered motility and migration by the JM mutation of *c-MET* would have significant impact on tumor cell invasion and metastatic potential. An *in vivo* model to further examine the significance of this pathway and the regulation of invasion and metastasis by JM mutation of c-MET would be warranted. It would also be useful to further identify the various individual cellular proteins, besides paxillin, with enhanced constitutive tyrosine phosphorylation in the JM mutants. Further work to clarify the role of the Sema domain mutation, and alternative transcripts of *c-MET* in HGF/c-MET signaling also promises to yield important insight into SCLC biology. This has important therapeutic implication for SCLC and we predict that small molecule inhibitors against c-MET or its mutated variants could be an effective targeted therapy against SCLC.

ACKNOWLEDGMENTS

We are grateful to Dr. George F. Vande Woude for providing c-*MET* and *TPR-MET* cDNA plasmids. We would like to thank Drs. Samuel C. Mok, Colin Koon, and Perry S. O. Chan for their help and advice in the project.

REFERENCES

1. Jemal, A., Murray, T., Samuels, A., Ghafoor, A., Ward, E., and Thun, M. J. Cancer statistics, 2003. CA Cancer J. Clin., *53:* 5–26, 2003.
2. Chute, J. P., Chen, T., Feigal, E., Simon, R., and Johnson, B. E. Twenty years of Phase III trials for patients with extensive-stage small-cell lung cancer: perceptible progress. J. Clin. Oncol., *17:* 1794–1801, 1999.
3. Salgia, R., and Skarin, A. T. Molecular abnormalities in lung cancer. J. Clin. Oncol., *16:* 1207–1217, 1998.
4. Kijima, T., Maulik, G., Ma, P. C., Tibaldi, E. V., Turner, R. E., Rollins, B., Sattler, M., Johnson, B. E., and Salgia, R. Regulation of cellular proliferation, cytoskeletal function, and signal transduction through CXCR4 and c-Kit in small cell lung cancer cells. Cancer Res., *62:* 6304–6311, 2002.
5. Wang, W. L., Healy, M. E., Sattler, M., Verma, S., Lin, J., Maulik, G., Stiles, C. D., Griffin, J. D., Johnson, B. E., and Salgia, R. Growth inhibition and modulation of kinase pathways of small cell lung cancer cell lines by the novel tyrosine kinase inhibitor STI 571. Oncogene, *19:* 3521–3528, 2000.
6. Maulik, G., Shrikhande, A., Kijima, T., Ma, P. C., Morrison, P. T., and Salgia, R. Role of the hepatocyte growth factor receptor, c-Met, in oncogenesis and potential for therapeutic inhibition. Cytokine Growth Factor Rev., *13:* 41–59, 2002.
7. Maulik, G., Kijima, T., Ma, P. C., Ghosh, S. K., Lin, J., Shapiro, G. I., Schaefer, E., Tibaldi, E., Johnson, B. E., and Salgia, R. Modulation of the c-Met/hepatocyte growth factor pathway in small cell lung cancer. Clin. Cancer Res., *8:* 620–627, 2002.
8. Jeffers, M., Rong, S., and Vande Woude, G. F. Enhanced tumorigenicity and invasion-metastasis by hepatocyte growth factor/scatter factor-met signalling in human cells concomitant with induction of the urokinase proteolysis network. Mol. Cell. Biol., *16:* 1115–1125, 1996.
9. Horiguchi, N., Takayama, H., Toyoda, M., Otsuka, T., Fukusato, T., Merlino, G., Takagi, H., and Mori, M. Hepatocyte growth factor promotes hepatocarcinogenesis through c-Met autocrine activation and enhanced angiogenesis in transgenic mice treated with diethylnitrosamine. Oncogene, *21:* 1791–1799, 2002.
10. Imai, J., Watanabe, M., Sasaki, M., Yamaguchi, R., Tateyama, S., and Sugano, S. Induction of c-*met* proto-oncogene expression at the metastatic site. Clin. Exp. Metastasis, *17:* 457–462, 1999.
11. Di Renzo, M. F., Olivero, M., Giacomini, A., Porte, H., Chastre, E., Mirossay, L., Nordlinger, B., Bretti, S., Bottardi, S., Giordano, S., *et al.* Overexpression and amplification of the *met/HGF* receptor gene during the progression of colorectal cancer. Clin. Cancer Res., *1:* 147–154, 1995.
12. Horikawa, T., Sheen, T. S., Takeshita, H., Sato, H., Furukawa, M., and Yoshizaki, T. Induction of c-*Met* proto-oncogene by Epstein-Barr virus latent membrane protein-1 and the correlation with cervical lymph node metastasis of nasopharyngeal carcinoma. Am. J. Pathol., *159:* 27–33, 2001.
13. Trusolino, L., and Comoglio, P. M. Scatter-factor and semaphorin receptors: cell signalling for invasive growth. Nat. Rev. Cancer, *2:* 289–300, 2002.
14. Petrelli, A., Gilestro, G. F., Lanzardo, S., Comoglio, P. M., Migone, N., and Giordano, S. The endophilin-CIN85-Cbl complex mediates ligand-dependent downregulation of c-Met. Nature (Lond.), *416:* 187–190, 2002.
15. Ma, P. C., Maulik, G., Christensen, J. G., and Salgia, R. c-*Met*: structure, functions and potential for therapeutic inhibition. Cancer Metastatic Rev., *22:* 309–325, 2003.
16. Schmidt, L., Duh, F. M., Chen, F., Kishida, T., Glenn, G., Choyke, P., Scherer, S. W., Zhuang, Z., Lubensky, I., Dean, M., Allikmets, R., Chidambaram, A., Bergerheim, U. R., Feltis, J. T., Casadevall, C., Zamarron, A., Bernues, M., Richard, S., Lips, C. J., Walther, M. M., Tsui, L. C., Geil, L., Orcutt, M. L., Stackhouse, T., Zbar, B., *et al.* Germline and somatic mutations in the tyrosine kinase domain of the *MET* proto-oncogene in papillary renal carcinomas. Nat. Genet., *16:* 68–73, 1997.
17. Schmidt, L., Junker, K., Weirich, G., Glenn, G., Choyke, P., Lubensky, I., Zhuang, Z., Jeffers, M., Vande Woude, G., Neumann, H., Walther, M., Linehan, W. M., and Zbar, B. Two North American families with hereditary papillary renal carcinoma and identical novel mutations in the *MET* proto-oncogene. Cancer Res., *58:* 1719–1722, 1998.
18. Schmidt, L., Junker, K., Nakaigawa, N., Kinjerski, T., Weirich, G., Miller, M., Lubensky, I., Neumann, H. P., Brauch, H., Decker, J., Vocke, C., Brown, J. A., Jenkins, R., Richard, S., Bergerheim, U., Gerrard, B., Dean, M., Linehan, W. M., and Zbar, B. Novel mutations of the *MET* proto-oncogene in papillary renal carcinomas. Oncogene, *18:* 2343–2350, 1999.
19. Salgia, R., Li, J. L., Ewaniuk, D. S., Pear, W., Pisick, E., Burky, S. A., Ernst, T., Sattler, M., Chen, L. B., and Griffin, J. D. BCR/ABL induces multiple abnormalities of cytoskeletal function. J. Clin. Investig., *100:* 46–57, 1997.
20. Angeloni, D., Danilkovitch-Miagkova, A., Ivanov, S. V., Breathnach, R., Johnson, B. E., Leonard, E. J., and Lerman, M. I. Gene structure of the human receptor tyrosine kinase RON and mutation analysis in lung cancer samples. Genes Chromosomes Cancer, *29:* 147–156, 2000.
21. Yu, J., Miehlke, S., Ebert, M. P., Hoffmann, J., Breidert, M., Alpen, B., Starzynska, T., Stolte Prof, M., Malfertheiner, P., and Bayerdorffer, E. Frequency of TPR-MET rearrangement in patients with gastric carcinoma and in first-degree relatives. Cancer (Phila.), *88:* 1801–1806, 2000.
22. Heideman, D. A., Snijders, P. J., Bloemena, E., Meijer, C. J., Offerhaus, G. J., Meuwissen, S. G., Gerritsen, W. R., and Craanen, M. E. Absence of tpr-met and

expression of c-met in human gastric mucosa and carcinoma. J. Pathol., *194:* 428–435, 2001.
23. Rong, S., Bodescot, M., Blair, D., Dunn, J., Nakamura, T., Mizuno, K., Park, M., Chan, A., Aaronson, S., and Vande Woude, G. F. Tumorigenicity of the *met* proto-oncogene and the gene for hepatocyte growth factor. Mol. Cell. Biol., *12:* 5152–5158, 1992.
24. Rong, S., Oskarsson, M., Faletto, D., Tsarfaty, I., Resau, J. H., Nakamura, T., Rosen, E., Hopkins, R. F., III, and Vande Woude, G. F. Tumorigenesis induced by coexpression of human hepatocyte growth factor and the human *met* protooncogene leads to high levels of expression of the ligand and receptor. Cell Growth Differ., *4:* 563–569, 1993.
25. Oskam, R., Coulier, F., Ernst, M., Martin-Zanca, D., and Barbacid, M. Frequent generation of oncogenes by *in vitro* recombination of *TRK* protooncogene sequences. Proc. Natl. Acad. Sci. USA, *85:* 2964–2968, 1988.
26. Salgia, R., Avraham, S., Pisick, E., Li, J. L., Raja, S., Greenfield, E. A., Sattler, M., Avraham, H., and Griffin, J. D. The related adhesion focal tyrosine kinase forms a complex with paxillin in hematopoietic cells. J. Biol. Chem., *271:* 31222–31226, 1996.
27. Jeffers, M., Schmidt, L., Nakaigawa, N., Webb, C. P., Weirich, G., Kishida, T., Zbar, B., and Vande Woude, G. F. Activating mutations for the met tyrosine kinase receptor in human cancer. Proc. Natl. Acad. Sci. USA, *94:* 11445–11450, 1997.
28. Lee, J. H., Han, S. U., Cho, H., Jennings, B., Gerrard, B., Dean, M., Schmidt, L., Zbar, B., and Vande Woude, G. F. A novel germ line juxtamembrane Met mutation in human gastric cancer. Oncogene, *19:* 4947–4953, 2000.
29. Meng, Q., Mason, J. M., Porti, D., Goldberg, I. D., Rosen, E. M., and Fan, S. Hepatocyte growth factor decreases sensitivity to chemotherapeutic agents and stimulates cell adhesion, invasion, and migration. Biochem. Biophys. Res. Commun., *274:* 772–779, 2000.
30. Phelps, R. M., Johnson, B. E., Ihde, D. C., Gazdar, A. F., Carbone, D. P., McClintock, P. R., Linnoila, R. I., Matthews, M. J., Bunn, P. A., Jr., Carney, D., Minna, J. D., and Mulshine, J. L. NCI-Navy Medical Oncology Branch cell line data base. J. Cell. Biochem. Suppl., *24:* 32–91, 1996.
31. Nakao, M., Yokota, S., Iwai, T., Kaneko, H., Horiike, S., Kashima, K., Sonoda, Y., Fujimoto, T., and Misawa, S. Internal tandem duplication of the *flt3* gene found in acute myeloid leukemia. Leukemia (Baltimore), *10:* 1911–1918, 1996.
32. Carney, D. N., Gazdar, A. F., Bepler, G., Guccion, J. G., Marangos, P. J., Moody, T. W., Zweig, M. H., and Minna, J. D. Establishment and identification of small cell lung cancer cell lines having classic and variant features. Cancer Res., *45:* 2913–2923, 1985.
33. Cooper, C. S., Park, M., Blair, D. G., Tainsky, M. A., Huebner, K., Croce, C. M., and Vande Woude, G. F. Molecular cloning of a new transforming gene from a chemically transformed human cell line. Nature (Lond.), *311:* 29–33, 1984.
34. Soman, N. R., Correa, P., Ruiz, B. A., and Wogan, G. N. The *TPR-MET* oncogenic rearrangement is present and expressed in human gastric carcinoma and precursor lesions. Proc. Natl. Acad. Sci. USA, *88:* 4892–4896, 1991.
35. Wybenga-Groot, L. E., Baskin, B., Ong, S. H., Tong, J., Pawson, T., and Sicheri, F. Structural basis for autoinhibition of the $EphB_2$ receptor tyrosine kinase by the unphosphorylated juxtamembrane region. Cell, *106:* 745–757, 2001.
36. Baxter, R. M., Secrist, J. P., Vaillancourt, R. R., and Kazlauskas, A. Full activation of the platelet-derived growth factor beta-receptor kinase involves multiple events. J. Biol. Chem., *273:* 17050–17055, 1998.
37. Irusta, P. M., and DiMaio, D. A single amino acid substitution in a WW-like domain of diverse members of the PDGF receptor subfamily of tyrosine kinases causes constitutive receptor activation. EMBO J., *17:* 6912–6923, 1998.
38. Hayakawa, F., Towatari, M., Kiyoi, H., Tanimoto, M., Kitamura, T., Saito, H., and Naoe, T. Tandem-duplicated Flt3 constitutively activates STAT5 and MAP kinase and introduces autonomous cell growth in IL-3-dependent cell lines. Oncogene, *19:* 624–631, 2000.
39. Regnauld, K., Nguyen, Q. D., Vakaet, L., Bruyneel, E., Launay, J. M., Endo, T., Mareel, M., Gespach, C., and Emami, S. G-protein α (olf) subunit promotes cellular invasion, survival, and neuroendocrine differentiation in digestive and urogenital epithelial cells. Oncogene, *21:* 4020–4031, 2002.
40. Zelivianski, S., Verni, M., Moore, C., Kondrikov, D., Taylor, R., and Lin, M. F. Multipathways for transdifferentiation of human prostate cancer cells into neuroendocrine-like phenotype. Biochim. Biophys. Acta, *1539:* 28–43, 2001.
41. Di Renzo, M. F., Olivero, M., Martone, T., Maffe, A., Maggiora, P., Stefani, A. D., Valente, G., Giordano, S., Cortesina, G., and Comoglio, P. M. Somatic mutations of the *MET* oncogene are selected during metastatic spread of human HNSC carcinomas. Oncogene, *19:* 1547–1555, 2000.
42. Sattler, M., Pisick, E., Morrison, P. T., and Salgia, R. Role of the cytoskeletal protein paxillin in oncogenesis. Crit. Rev. Oncog., *11:* 63–76, 2000.
43. Sattler, M., and Salgia, R. Role of the adapter protein CRKL in signal transduction of normal hematopoietic and BCR/ABL-transformed cells. Leukemia (Baltimore), *12:* 637–644, 1998.
44. Liu, Y. The human hepatocyte growth factor receptor gene: complete structural organization and promoter characterization. Gene (Amst.), *215:* 159–169, 1998.
45. Wang, Z., Lo, H. S., Yang, H., Gere, S., Hu, Y., Buetow, K. H., and Lee, M. P. Computational analysis and experimental validation of tumor-associated alternative RNA splicing in human cancer. Cancer Res., *63:* 655–657, 2003.
46. Modrek, B., and Lee, C. A genomic view of alternative splicing. Nat. Genet., *30:* 13–19, 2002.
47. Lee, C. C., and Yamada, K. M. Identification of a novel type of alternative splicing of a tyrosine kinase receptor. Juxtamembrane deletion of the c-met protein kinase C serine phosphorylation regulatory site. J. Biol. Chem., *269:* 19457–19461, 1994.
48. Lee, C. C., and Yamada, K. M. Alternatively spliced juxtamembrane domain of a tyrosine kinase receptor is a multifunctional regulatory site. Deletion alters cellular tyrosine phosphorylation pattern and facilitates binding of phosphatidylinositol-3-OH kinase to the hepatocyte growth factor receptor. J Biol Chem, *270:* 507–510, 1995.
49. Goshima, Y., Ito, T., Sasaki, Y., and Nakamura, F. Semaphorins as signals for cell repulsion and invasion. J. Clin. Investig., *109:* 993–998, 2002.
50. Kagoshima, M., and Ito, T. Diverse gene expression and function of semaphorins in developing lung: positive and negative regulatory roles of semaphorins in lung branching morphogenesis. Genes Cells, *6:* 559–571, 2001.
51. Roche, J., Boldog, F., Robinson, M., Robinson, L., Varella-Garcia, M., Swanton, M., Waggoner, B., Fishel, R., Franklin, W., Gemmill, R., and Drabkin, H. Distinct 3p21.3 deletions in lung cancer and identification of a new human semaphorin. Oncogene, *12:* 1289–1297, 1996.
52. Morotti, A., Mila, S., Accornero, P., Tagliabue, E., and Ponzetto, C. K252a inhibits the oncogenic properties of Met, the HGF receptor. Oncogene, *21:* 4885–4893, 2002.
53. Sattler, M., Pride, Y. B., Ma, P. C., Gramlich, J. L., Chu, S. C., Quinnan, L. A., Shirazian, S., Liang, C., Podar, K., Christensen, J. a., and Salgia, R. A novel small molecule Met inhibitor induces apoptosis in cells transformed by the oncogenic *TPR-MET* tyrosine kinase. Cancer Res., *63:* 5462–5469, 2003.